Evolution of the tempered lath structure of the 12%Cr steels with low N and high B contents during creep

Evolution of the tempered lath structure of the 12%Cr steels with low N and high B contents during creep

A E Fedoseeva[1*], I S Nikitin[1], A E Fedoseev[1], R O Kaibyshev[1]

[1]Belgorod National Research University, Pobeda 85 308015 Belgorod, Russia

[*]Corresponding author: fedoseeva@bsu.edu.ru

Abstract. 9-12%Cr martensitic steels are promising materials for elements of boilers, tubes, pipes, heaters and steam blades for fossil power plants, which are able to operate at ultra-supercritical parameters of steam. Creep tests were carried out for two 12%Cr and 9%Cr steels at 650°C. After tempering at 750-770°C, a tempered lath structure was revealed in all the steels studied. The 12%Cr-Ta steel had the smallest lath width among the steels studied that provided the longest creep rupture time after creep test at 650°C/120 MPa. During creep, the applied stress causes the lath growth and the formation of subgrains instead of martensitic laths. The experimental sizes of subgrains and equilibrium subgrains, calculated on balance of driving and retarding forces and using the dependence of the size of subgrains on the applied stress during creep, were compared to estimate the contributions of secondary particles and applied stress to the growth of subgrains during tempering and creep in the different steels.

1. Introduction

12%Cr martensitic steels are considered to be materials for the elements of steam blades in fossil power plants operating at ultra-supercritical parameters of steam [1-2]. The main disadvantage of 12%Cr martensitic steels is the low structural stability during creep at elevated temperatures, i.e. the tempered martensite lath structure (TMLS) evolves fast into a subgrain structure [2]. This reduces the creep resistance of 12%Cr steels and limits their application in fossil power plants [1,2]. 9%Cr steels usually demonstrate high structural stability for long-term thermal exposure that provides high creep resistance [3-5]. A new approach to alloying of 9-12%Cr steels, which consists in adding Co, decreasing the N content, and increasing the B content [6-10], can eliminate the poor structural stability of the 12%Cr steel during creep. The addition of Co increases the volume fraction of the secondary phase particles and contribute to the solid solution strengthening [3,4,6]. Decreasing N content together with increasing B content eliminates the formation of coarse BN nitrides and slows down the particle coarsening [7-9]. Additionally, new 12%Cr steels contain 0.8%Cu and 0.07%Ta as austenite-stabilizing elements [9]. Moreover, Cu acts as nucleation sites for Laves phase [7-9]. The aim of this study is to report the evolution of the tempered martensite lath structure of two Co-containing 12%Cr steels with low N and high B contents during creep at 650°C in comparison with a 9%Cr steel containing Co with standard N and B contents [4].

2. Experimental procedure

Two 12% Cr steels, denoted here as 12%Cr and 12%Cr-Ta, were prepared by vacuum induction melting, and a 9% Cr steel, denoted here as 9%Cr, was prepared by air induction melting. The chemical compositions of the Co-containing 12%Cr steels with low N and high B contents and the 9%Cr steel with standard N and B contents are listed in Table 1.

Table 1. Chemical compositions of 12%Cr and 9%Cr steels.

	C	Cr	Co	Mo	W	V	Cu	Nb	B	N	Ta
12%Cr	0.09	11.3	3.9	0.63	2.4	0.24	0.78	0.07	0.009	0.003	-
12%Cr-Ta	0.11	11.4	3.0	0.62	2.5	0.23	0.76	0.04	0.01	0.003	0.07
9%Cr	0.10	9.5	3.0	0.5	1.8	0.20	-	0.05	0.005	0.05	-

All steels were solution treated at 1050-1070°C for 1 h, cooled in air, and subsequently tempered at 750-770°C for 3 h. Cylindrical specimens with a gauge length of 60 mm and a diameter of 6 mm were crept until rupture at 650°C under applied stresses of 180-100 MPa with a step of 20 MPa. A JEOL–2100 transmission electron microscope (TEM) was used for structural characterization of tempered and crept structures [3-5]. The volume fractions of the secondary phase particles were calculated using the Thermo-Calc software [3-5].

3. Results and Discussion

3.1 Tempered state

The microstructures of the Co-containing 12%Cr and 9%Cr steels after heat treatment, obtained by TEM are represented in Figure 1. The microstructural parameters after heat treatment for both steels are summarized in Table 2.

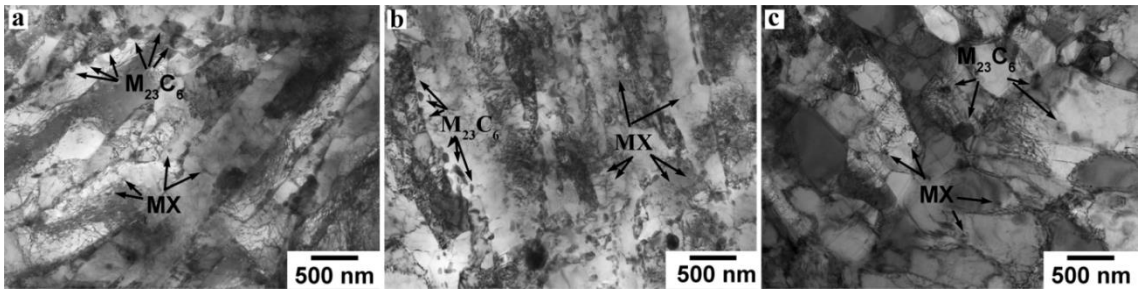

Figure 1. TMLS of the 12%Cr (a), 12%Cr-Ta (b) and 9%Cr (c) steels after heat treatment.

Table 2. Structural parameters of the 12%Cr and 9%Cr steels after heat treatment.

	PAG size, μm	Fraction of δ-Fe,%	Lath width, nm	Dislocation density, m^{-2}	Particle size, nm		Volume fraction, %	
					$M_{23}C_6$	MX	$M_{23}C_6$	MX
12%Cr	51±2	6±1	305±30	1.3×10^{14}	61±5	29±3	1.59	0.06
12%Cr-Ta	48±2	9±2	285±30	2.0×10^{14}	55±5	20±3	1.81	0.07
9%Cr	10±1	0	380±30	2.0×10^{14}	90±5	30±3	1.80	0.25

After tempering at 750-770°C, a tempered martensite lath structure (TMLS) was observed in both 12%Cr martensitic steels (Figure 1a,b), whereas a mixture of TMLS and subgrain structure was revealed in the 9%Cr steel (Figure 1c). The width of the martensitic laths in all steels was similar and comprised 300-400 nm, whereas the dislocation density in the 12%Cr steel was lower than that in the 12%Cr-Ta and 9%Cr steels (Table 2). In all steels, Cr-rich $M_{23}C_6$ carbides are located at grain boundaries and V-, Nb- or Ta-rich MX carbonitrides randomly distributed in the matrix (Figure 1). The mean size of $M_{23}C_6$ particles in the 9%Cr steel was significantly larger than that in the 12%Cr steels (Figure 1, Table 2), whereas the mean size of MX carbonitrides was similar in all steels.

3.2 Creep properties

Figure 2 shows the creep rupture data of the steels at a temperature of 650°C. Both 12%Cr steels did not demonstrate any breakdown in the curve "Applied stress vs. Time to rupture", whereas a creep strength breakdown appeared in the 9%Cr steel after 2000 h of creep tests (Figure 2a). The addition of Ta, as well as a decrease in the N content to 0.003% together with an increase in the B content to 0.012 wt.% affects positively the creep rupture strength (Figure 2a). A decrease in the minimum creep rate and an increase in the time to rupture took place (Figure 2b).

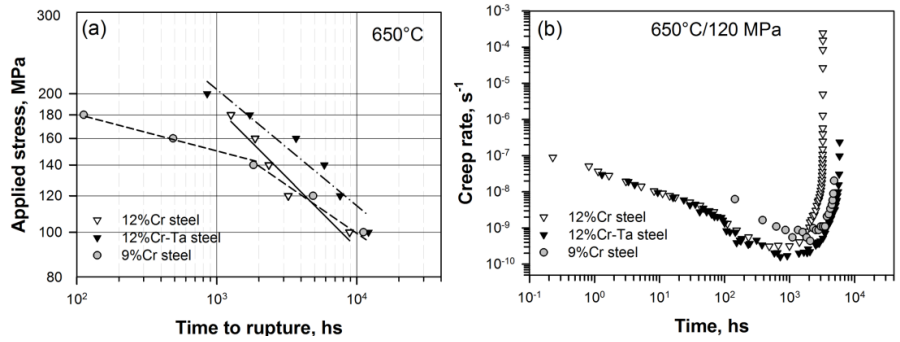

Figure 2. Time to rupture vs. stress curves (a) and minimal creep rate vs. time curves (b).

3.3 Evolution of TMLS during creep

After the creep test at 650°C/120 MPa, the microstructures of all steels strongly evolved. The TMLS partially transformed into a subgrain structure with a mean size of subgrains of 0.7 μm in the 12%Cr steels (Figure 3a,b); a 100% subgrain structure with a mean subgrain size of 1.4 μm instead of the TMLS was revealed in the 9%Cr steel (Figure 3c). The dislocation density in all steels decreased to 10^{13} m^{-2}. Grain boundary $M_{23}C_6$ and Laves phase particles and MX carbonitrides coarsened, especially, in the 9%Cr steel (Table 3). No evidence of Z-phase particles was observed in all of the steels studied.

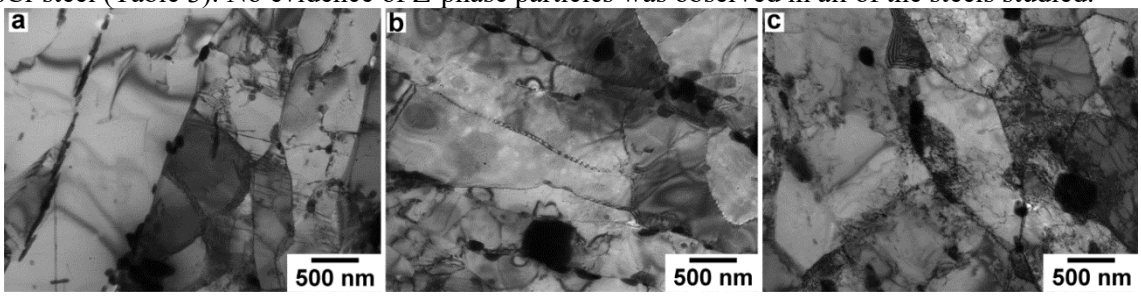

Figure 3. Evolution of TMLS in the 12%Cr (a), 12%Cr-Ta (b) and 9%Cr (c) steels after creep test at 650°C/120 MPa.

Table 3. Structural parameters of the 12%Cr and 9%Cr steels after creep test at 650°C/120 MPa.

	Lath width, nm	Subgrain size, nm	Dislocation density, m^{-2}	Particle size, nm			Volume fraction, %		
				$M_{23}C_6$	Laves	MX	$M_{23}C_6$	Laves	MX
12%Cr	665±30	760±30	0.8×10^{14}	109±5	170±5	45±3	1.68	2.10	0.06
12%Cr-Ta	650±30	645±30	0.7×10^{14}	96±5	197±5	37±3	2.07	2.10	0.07
9%Cr	-	1400±30	0.4×10^{14}	200±5	280±5	70±3	1.96	1.32	0.25

The equilibrium subgrain size *D,* which may be achieved during creep, can be estimated (1) on the assumption of the driving and retarding forces are in a balance [3] and (2) using the dependence of

the subgrain size on the applied stress during creep [2]. The calculated and experimental values of the subgrain size in the steels studied are represented in Table 4.

Table 4. Calculated and experimental values of the subgrain size.

	Tempered state		Crept state		
	D [3], μm	D_{exp}, μm	D [3], μm	D_{∞} [2], μm	D_{exp}, μm
12%Cr	0.33	0.31	0.57	1.24	0.76
12%Cr-Ta	0.27	0.29	0.49	1.24	0.65
9%Cr	0.41	0.38	0.92	1.24	1.40

The experimental subgrain sizes after tempering in all steels are in accordance with the equilibrium values estimated from the balance between the driving and retarding forces [3] (Table 4). The largest subgrain size in the 9%Cr steel is caused by the low Zener pressure from the particles due to their large size (Table 2). The smallest subgrain size of 0.27 μm occurs in the 12%Cr-Ta steel that is attributed to the finest particle sizes and the highest volume fraction of $M_{23}C_6$ carbides (Table 2).

After creep tests, the equilibrium subgrain sizes, estimated from the balance between driving and retarding forces, are insignificantly smaller than the experimental subgrain ones with the exception of the 9%Cr steel (Table 4). Boundary particles in the 12%Cr steels effectively prevent the lath growth, resulting in smaller experimental subgrain sizes than those calculated using the dependence of the subgrain size on the applied stress [2], though the applied stress leads to a strong evolution of the TMLS accelerating the migration of lath boundaries [2,7-9]. In the 9%Cr steel, the secondary particles do not control the lath growth during long-term creep that probably causes a breakdown of the creep strength [4]. An insignificant lath growth in the 12%Cr steels provides no creep strength breakdown appearance (Figure 2a). The 12%Cr-Ta steel demonstrates the longest creep rupture time in a creep condition of 650°C/120 MPa (Figure 2) that can be attributed to the remaining TMLS and the finest subgrain sizes.

4. Conclusions

The formation of a TMLS in all 12%Cr and 9%Cr steels during tempering at 750-770°C was revealed. The smallest lath width was observed in the 12%Cr-Ta steel, since fine boundary particles ensured, effective retarding of the lath boundary migration. During creep, the TMLS strongly evolves in all steels; the applied stress provides the formation of subgrains. However, the boundary particles effectively prevent subgrain growth in the 12%Cr steels compared with the 9%Cr steel.

Acknowledgments

The study was financially supported by Ministry of Science and Higher Education of the Russian Federation, the President's Grant for PhD – young scientists (grant number 075-15-2019-1165).

References

[1] Kern T U, Staubli M, Scarlin B 2002 *ISIJ International* **42** 1515
[2] Hald J, Korcakova L 2003 *ISIJ International* **43** 420
[3] Fedoseeva A, Kozlov P, Dudko V, Skorobogatykh V, Shchenkova I, Kaibyshev R 2015 *Phys. Met. Metall.* **116** 1047
[4] Fedoseeva A, Dudova N, Kaibyshev R 2016 *Mater. Sci. Eng. A* **654** 1
[5] Dudko V, Fedoseeva A, Belyakov A, Kaibyshev R 2015 *Phys. Met. Metall.* **116** 1165
[6] Helis L, Toda Y, Hara T, Miyazaki H, Abe F 2009 *Mater. Sci. Eng. A* **510–511** 88
[7] Abe F 2011 *Procedia Engineering* **10** 94
[8] Hald 2008 *J Int J Pres Ves Pip* **85** 30
[9] Klueh R L 2005 *International Materials Reviews* **50** 287